The Application of Non-linear Dynamics Methods for Radar Target Identification

F. J. Rachford and T. L. Carroll
US Naval Research Laboratory, USA

Abstract— Currently radar target identification is effected by finding the downrange distribution of scatterers on a platform using high definition radar and referencing this distribution to a look-up table of measured radar returns. This method is difficult due to the rapid scintillation of the radar signal of a flying target at short wavelengths. We investigate a method of target identification in the low definition, relatively long wavelength, limit using techniques derived from the field of non-linear dynamics. In this limit the radar reflection is much less sensitive to the orientation of the target to the radar and scintillation is greatly reduced. Modern detection advances allow the digitization and processing of raw real time non-pulse compressed waveforms. We simulate the raw radar returns from several very similar small (4 to 5 wavelength) objects (i.e., cylinder, cone-cylinder, cone-ogive and double ogive) illuminated with chaotic or random modulated waveforms or a linear chirp using a commercial finite difference time domain code. In this aggressive limit we embed the target return in two dimensions using the method of delays to form an attractor. The geometric properties of the attractors are analyzed to distinguish between these similar target objects in the low definition limit. Our method selects random points on a reference attractor (or strands of points) with many Euclidean nearest neighbors and compares these with the nearest neighbor density of points (or strands) with the same time index on an attractor from an unknown target. Comparing the density of nearest neighbors at these points on two attractors allows us to calculate probabilities of correct identification. (Is the unknown signal from the reference target or from one of the other targets?) Simulation data and analyses derived from three different transmit waveforms are compared. The robustness of our target ID method is probed by the addition of white noise to the signals.

1. INTRODUCTION

In radar, a microwave wave train interacts with a complex target and is reflected to a detector. Conventional processing is used to locate the illuminated target in space ($c \times \Delta t/2$) and determine its velocity [1]. Determining the identity of the target and distinguishing one target from similar targets has proven more of a challenge [2]. Present target identification (ID) methods include using high frequency waveforms and pulse compression to find the distribution of down range locations of scatterers [3] on a complex target or studying the decay of characteristic resonant excitations [4–6]. A target is identified by matching the scatterer locations or characteristic resonances with a lookup table of measured values. The return from high frequency/high definition radar is very sensitive to target aspect and dynamic flexing leading to ambiguities in identification. Resonant ring down returns are less susceptible to aspect or dynamics of the target structure but rapidly decay and are very difficult to detect in real operational environments. Other approaches to target identification use adaptive waveform design [7–11]. In this paper we describe a method for target identification that we have recently developed [12–15] and look at its dependence on several candidate radar waveforms in the presence of Gaussian noise. To make the identification process especially challenging we choose to illuminate four very similar simple targets, Fig. 1, roughly four and a half wavelengths long by a bit more than one wavelength in diameter. We simulate the radar process using a commercial [16] finite difference time domain (FDTD) code [17].

2. WAVEFORM CONSTRUCTION

Three waveforms were constructed to illuminate the targets by concatenating one thousand individual sinusoids with varying periods. The periods of these frequency modulated CW waveforms were constrained to fall in a 400 MHz bandwidth with center frequency of 2 GHz and were selected according to three different rules: a linearly increasing frequency chirp, the output of a low dimensional chaotic map and a pseudo random number sequence. The low dimensional chaotic map used to construct the chaotically modulated wave train is described by

$$z(n+1) = 2.1 z(n) \mod 1 \tag{1}$$

the linear chirp follows $z(n+1) = z(n) + 0.001, z(0) = 0.001$, and the random sequence by $z(n) = ran(n)$. Each frequency modulated signal was then created from a series of concatenated sinusoids, with the frequency of the n'th sinusoid determined by $\zeta(n) = 1.0 + \beta(z(n) - 0.5)$, where β was used to vary the modulation bandwidth. The sinusoids were matched in phase when one sinusoid ended and the other began. Mathematically, the nth sinusoid of $\mathbf{s}$ was given by

$$s\left(i\right) = \sin\left(2\pi t / \left[600\zeta\left(n\right)\right]\right) \quad \left[i = 0, 1, 2 \ldots, i < 600\zeta\left(n\right)\right] \tag{2}$$

If $\zeta(n) = 1$, then the initial period of the sinusoid was 600 points. The random waveform was generated similarly except the chaotic map was replaced by a pseudo random number generator. The chirp was generated by a linearly incremented number sequence. All waveforms were later resampled and scaled to fall within the prescribed center frequency and bandwidth for presentation to the FDTD code.

3. IDENTIFICATION METHOD

One can view the process of scattering an electromagnetic wave from a target as a filter acting on a signal. In general there is no continuous function that can reverse the effects of a filter and reconstruct the input waveform. Also there is no continuous function relating the outputs of two different filters excited by the same waveform. Since the scattering process here is deterministic, dynamical systems theory applies and can be used to calculate the probability that two received signals can be related by a function and, hence, have been scattered from the same target [18]. We emphasize we are working here with raw scattered waveforms. Simple techniques such as signal averaging can be tolerated but no matched filtering or pulse compression is applied upon detection. (Some band pass filtering is tolerable as long as it is applied equally to all signals under consideration.)

We assume that once a target of interest has been located and characterized by conventional methods that real time digitized waveforms of the return signal are available for analysis and that the waveforms can be corrected for Doppler effects by appropriate resampling. Our method proceeds by embedding the digitized normalized, non pulse compressed waveform, $s(i)$, in two dimensions by the method of delays [19–22]. We do this by constructing the set of delay vectors $\mathbf{S}(i)$:

$$\mathbf{S}\left(i\right) = \left[s\left(i\right), s\left(i+\tau\right)\right] \tag{3}$$

where the delay time τ_j is by known methods [21, 22]. The set of these vectors over time form a reconstruction (also called an embedding) of the signa lin a phase space. The trajectory of these vectors carry information about the waveform interaction with the target. To discriminate between targets we look at the average Euclidean separation between nearest neighbor vectors on a reference target and compared with the average separation of the same vectors on embedded return signals from "unknown" targets. The process is initiated by selecting random points on the reference target embedding (attractor), finding their nearest neighbor points on different cycles (sufficiently separated in time) and calculating the average neighbor separation for the collection of initial seed locations. These same points and their neighbors are located in time on the "unknown" signal embedding and their average separation is recorded. In practice instead of using individual points, we use strands of 128 temporarily adjacent points in the embedding. Using strands makes the analysis less sensitive to additive noise by an effective signal averaging that takes place in the strand separation calculation. Strands also mitigate small inaccuracies in the loction of reference strands in the "unknown" signal. We expect that targets that are similar to the reference target will have comparably smaller average nearest neighbor strand separations in their embedded return signals than would be the case for targets with more differing geometries. This in fact is what we find and we used this effect realize our target identification.

4. TARGETS AND SIMULATION

The four electrically small perfectly conductive targets simulated in this work are shown in Figure 1. All axially symmetric shapes have a maximum diameter of 18 cm and the *cylinder, double ogive* and *cone cylinder* targets are 67 cm long whereas *cone ogive* is 74 cm long. All the targets are electrically small since the waveform center frequency is 2 GHz, 15 cm. In the FDTD simulation the targets were rotated +10° (nose up) in elevation and the mono-static return was scanned 60° in azimuth beginning with 0° azimuth facing the elevated ends. We rotated the targets +10° elevation to avoid the 0° specular flash off the flat end of the cylinder. The electric polarization was in the azimuthal

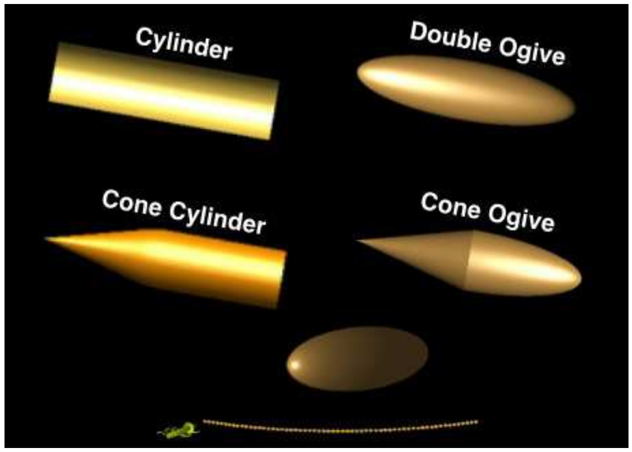

Figure 1: The four FDTD simulated shapes used in this study. All the objects simulated in this paper are 18 cm in diameter and the double ogive, cylinder and the cone ogive are all 67 cm long while the cone cylinder is 74 cm long. The objects are pitched +10° in elevation and are rotated in one degree increments from 0° (nose forward) to 60° in azimuth. The impinging waveform is polarized in the plane of the scan.Very similar results are seen when taking any of the other targets as reference. The best separation between target and other shape data occurs employing the chaotic waveform.

plane of the scan and data was taken at 1° intervals. 60000 FDTD time steps were executed at each degree and the back-scattered signal was low pass filtered at 3 GHz to reduce any accumulating digitizing errors.

The analysis proceeds by selecting and normalizing 50000 data points in each data set centered on the reflection from the target. The normalization was necessary since the amplitude of the return signals depends on the orienttion and shape of each target. An average normalization places all signals on the same scale independent of target. Each signal is embedded in two dimensions by the method of delays with, in this case, the delay being 13 points or about a quarter of an average sinusoid cycle. One target is chosen as reference and 100 random strands are placed at random sites in the embedded data for each angle. At each test strand 5 nearest neighbor strands are located and their average separation from each original strand is noted. The average of the average nearest neighbor distances from all 100 seeded strands is then found. The embedded data from one of the four targets is then seeded with strands and positioned at the same location as the initial and nearest neighbor strand locations on the reference target. The strand separation of each of the seed strands and its associated neighbors now located in the new embedding are measured and averaged. This process is repeated for each angle and then again for each waveform. All four targets serve as reference targets in turn to complete our analysis.

The strand separation versus angle for the case of the three waveforms and four unknown targets with the cylinder data taken as the reference is shown in Figure 2. Since here the reference was the cylinder, the lowest curve corresponding to the smallest average strand separation at each angle belongs to the cylinder case (red curve noted in the legend NC for new cylinder). For the case of the chaoticly modulated waveform the other three targets result in curves that are well separated from the cylinder trace. The cone cylinder (CC) and the cone ogive share (CO) the same cone on their "front" ends and their traces overlap using the cylinder reference. When using either one as reference they are well separated and distinguishable. In the case of the randomly modulated waveform the three are largely separated from the cylinder curve but are not as well separate as in the previous case. Finally for the chirp waveform, the cylinder curve and the cone cylinder and cone ogive strand separations are much closer and overlap at larger angles while only the double ogive (DO) data is well separated from the cylinder. In this case it would be difficult to distinguish the cylinder from the cone cylinder or cone ogive. In the case of the chirp similar bunching of curves is seen with the other targets taken as reference.

Addition of Gaussian Noise: To test the susceptibility of our method to noise, we add various amounts of Gaussian noise to our unknown signals. Our signals are normalized to an average amplitude of 1. The noise is added to the signal point by point at maximum amplitudes ranging from 0.01 to 10 and then the summed signal is renormalized to to an average amplitude of 1. For each noise value all the calculations are rerun and at each angle a determination is made

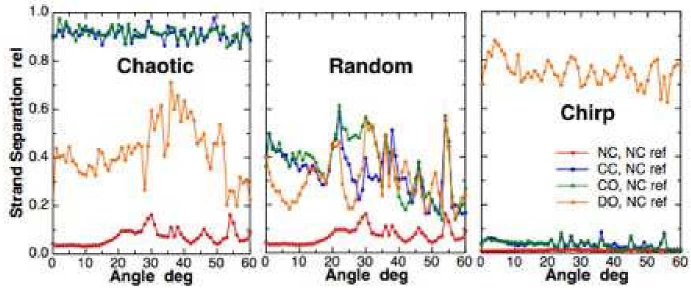

Figure 2: Three plots of strand separation versus angle for the case of the cylinder data serving as reference in the presence of zero additive noise for the cases of chaotic, random and chirp waveforms. Nearest neighbor strand locations chosen for the reference object are evaluated for data created using the each of the targets. In the legend NC = Cylinder, CC = Cone Cylinder, CO = Cone Ogive and DO = Double Ogive.

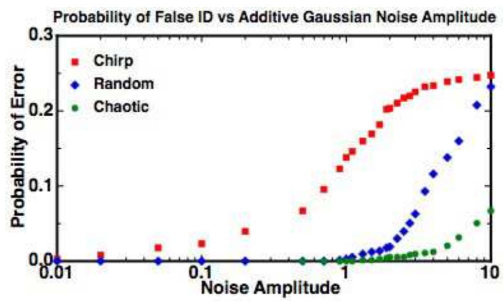

Figure 3: Probability of error in determining which of 4 shapes is present, as a function of added Gaussian noise level. Chaotic, random and chirp waveforms were reflected from the four objects. Comparisons of phase space strand separation occured at every one degree increment between 0° and 60° in azimuth.

if the test case strand separation value is greater or less than that of the correct trace. Where the correct trace was calculated by adding the same amount of noise to the reference signal and treating it as an unknown. To calculate the probability of error in the presence of noise we log an error every time the wrong target unknown produces a strand separation less that that calculated for the correct target. The number of errors are summed and normalized to the number of trials at risk over all angles and targets and target references. The probability of error is plotted versus noise in Figure 3 for each of the three waveform types.

5. DISCUSSION

It is clear that the type of waveform modulation strongly influences the utility of our target ID technique. (See Figure 2 and Figure 3.) The chaotically modulated waveform produces a clear separation between reference and "false" target strand separation traces at zero added noise that persists as noise is added to the signal. In the case of the chirp waveform, the nearest neighbor strands tend to cluster together in time as the period of sinusoids is gradually shorten and each cluster effectively samples less of the total waveform target interaction. For random modulation the rapid variation of periods leads to blur the target interaction modulations imposed on the return waveforms. The low dimensional chaotic modulation clearly works best in this application. With the addition of noise, all the strand separations increase and separate target curves begin to overlap resulting in false identifications. For waveforms that do not produce large separations in zero noise, the addition of noise quickly causes overlapping of strand separation traces and false lDs.

We envision using this method in conjunction with conventional pulse compression to initially locate targets of interest. From time of flight and location data and the target aspect can be estimated. The target can then be queried with a low dimensional chaotic modulated waveform and the real time non-pulse compressed waveform can be detected and processed. Signal averaging and band pass filtering can reduce the noise amplitude of the raw return signal. At that point an estimate of the residual noise level can be made and a library of target of interest low noise waveforms can have noise added for comparison with the unknown signal. Finally a probability of identity should be possible in a fully deployed system assuming the availability of a library of return waveforms from a variety of targets of interest.

Clearly this method is transmission waveform dependent. Though our particular single parameter shift register chaotic map works as a waveform generator, there are probably even better waveform constructs that can do the job. It may be possible to optimize the waveform to the specific target for further assurance.

6. CONCLUSION

We have shown that using the methods of time series embedding and nearest neighbor search drawn from non-linear dynamics, we can distinguish between very similar targets sized in the few wavelength regime. This method is strongly waveform dependent. We find that a waveform assembled by the concatenation of sinusoids prescribed by a simple chaotic single parameter shift register map is superior to a simple linear chirp or random waveform. Our method is shown to be robust in the presence of added Gaussian noise in the case of the chaotic waveform.

REFERENCES

1. Knott, E. F., J. F. Shaeffer, and M. T. Tulley, *Radar Cross Section*, Artech House, Norwood, MA, 1993.
2. Rihaczek, A. W. and S. J. Hershkowitz, *Theory and Practice of Radar Target Identification*, Artech House, Norwood, MA, 2000.
3. Hu, R. and Z. Zhu, "Researches on radar target classification based on high resolution range profiles," *Proc. IEEE*, Vol. 2, 951–955, 1997.
4. Berni, A. J., "Target identification by natural resonance estimation," *IEEE Transactions on Aerospace and Electronic Systems*, Vol. 11, 147–154, Feb. 1975.
5. Baum, C. E, E. J. Rothwell, K. M. Chen, and D. P. Nyquist, "The singularity expansion method and its application to target identification," *Proc. IEEE*, Vol. 79, 1481–1491, Oct. 1991.
6. Kennaugh, E., "The K-pulse concept," *IEEE Transactions on Antennas and Propagation*, Vol. 29, 327–331, 1981.
7. Pillai, S. U., H. S. Oh, D. C. Youla, and J. R. Guerci, "Optimum Transmit & receiver design in the presence of signal-dependent interference and channel noise," *IEEE Transactions on Information Theory*, Vol. 46, No. 2, 577–584, 2000.
8. Bergin, J. S., P. M. Techau, J. E. D. Carlos, and J. R. Guerci, "Radar waveform optimization for colored noise mitigation," *2005 IEEE Intrnational Radar Conference*, 149–154, 2005.
9. Vespe, M., C. J. Baker, and H. D. Griffiths, "Automatic target recognition using multi-diversity radar," *IET Radar, Sonar & Navigation*, Vol. 1, No. 6, 470–478, 2007.
10. Carroll, T. L., "Optimizing chaos-based signals for complex radar targets," *Chaos*, Vol. 17, 033103, 2007.
11. Rachford, F. J. and T. L. Carroll, "A chaos based waveform approach to radar target identification," *PIERS Online*, Vol. 6, No. 5, 476–479, 2010.
12. Carroll, T. L. and F. J. Rachford, "Nonlinear dynamics method for target identification," *Proceedings of SPIE*, Vol. 8021, 8021L1-1–8021L1-13, 2011.
13. Carroll, T. L. and F.J. Rachford, "Using filtering effects to identify objects," *Chaos: An Interdisciplinary Journal of Nonlinear Science*, Vol. 22, 023107–023109, Feb. 2012.
14. Carroll, T. L. and F. J. Rachford, "Object identification based on filtering," *IET-RSN*, Vol. 2013, 1–6, 2013.
15. Carroll, T. L. and F. J. Rachford, "Target identification based on state space analysis," *IEEE-RADAR*, Vol. 2014, 0032–0037, 2014.
16. XFDTD, Remcom Inc., State College, PA.
17. Taflove, A. and S. C. Hagness, *Computational Electrodynamics: The Finite Difference Time Domain Method*, Artech House, Norwood, MA, 2005.
18. Pecora, L. M., T. L. Carroll, and J. F. Heagy, "Statistics for mathematical properties between time series embeddings," *Physical Review E*, Vol. 52, 3420–3439, 1995.
19. Takens, F., *Dynamical Systems and Turbulence*, Springer, Berlin, 1981.
20. Sauer, T., J. A. Yorke, and M. Casdagli, "Embedology," *Journal of Statistical Physics*, Vol. 65, 579–616, Mar.–Apr. 1991.
21. Abarbanel, H. D. I., R. Brown, J. J. Sidorowich, and L. S. Tsmring, "The analysis of observed chaotic data in physical systems," *Reviews of Modern Physics*, Vol. 65, 1331–1392, Apr. 1993.
22. Pecora, L. M., L. Moniz, J. Nichols, and T. L. Carroll, "A unified approach to attractor reconstruction," *Chaos*, Vol. 17, 013110–013119, Jan. 2007.